Proceedings of the ASME 2018 Pressure Vessels and Piping Conference
PVP2018
July 15-20, 2018, Prague, Czech Republic

PVP2018-85120

COMPARISON OF PREDICTED CYCLIC CREEP DAMAGE FROM A MULTI-MATERIAL WELDMENT FEA MODEL AND THE TRADITIONAL R5 VOLUME 2/3 WELDMENT APPROACH

Feras ElAgha
WS Atkins Ltd.
Bristol, UK

David Tanner
WS Atkins Ltd.
Bristol, UK

David Knowles
WS Atkins Ltd. / University of Bristol
Bristol, UK

ABSTRACT

The R5 assessment procedure for Integrity of High Temperature Structures employs a Weld Strain Enhancement Factor (WSEF) (dependent only upon classified weld type) for predicting creep-fatigue crack initiation at weldments (V2/3 Appendix 4). This serves to amplify the calculated total strain at the weld toe for full penetration welds to account for geometric concentration and material mismatch between weldment zones. The value of WSEF recommended for fillet welds was derived from a review of a limited number of tests on thin welds which were not wholly representative of a typical fillet weld.

The objective of this paper is to present a comparison of the predicted cyclic creep defect initiation damage at a fillet weld toe using a multi-material finite element (FE) model of the weldment, against the damage predicted using the traditional R5 V2/3 approach, which uses only the parent material properties to derive the weld toe strain range in combination with the WSEF. In this example, the fillet weld joins a high temperature tube to an anti-vibration strap. There is pressure loading in the tube and displacement loading due to thermal expansion.

The FE model incorporates material properties associated with both the parent and the weld metal, including elastic modulus, plastic yield properties, creep deformation, and creep ductility (to determine damage via ductility exhaustion). The finite element analysis is run for 30 cycles (pressure and thermal cycling) with an average dwell period of 736 hours, with predicted damages for 100 cycles estimated using extrapolation. Sensitivities considering the stress-strain properties of the weld are included.

The cycle to cycle evolution of damage after 100 cycles including the weld-parent interaction in the FE modelled weldment is shown to be significantly lower than that predicted by the traditional R5 V2/3 route.

NOMENCLATURE

WSEF	Weld Strain Enhancement Factor
FEA	Finite Element Analysis
SCF	Stress Concentration Factor
HAZ	Heat Affected Zone
Z	Elastic Follow-up Factor

INTRODUCTION

Finite element analysis (FEA) is typically utilised in an R5 V2/3 [1] creep-fatigue initiation assessment of weldments to provide linearised elastic stresses via a monotonic homogenous (parent) material analysis. The assessment combines these FEA outputs with conservative assumptions regarding the weld details via stress/strain factors (i.e. a combined geometric concentration and material mismatch weld strain enhancement factor (WSEF) and an additional geometric stress concentration factor (SCF), if required) and simplified load cycles to derive a stabilised position when shakedown is demonstrated. The resulting strain range is used to determine fatigue damage and a ductility exhaustion approach is used to calculate creep damage

during high temperature dwells. A detailed description of the R5 V2/3 assessment route for weldments is shown in [3].

The intent of this route is to offer a simplified and conservative calculation to easily assess numerous components. Unfortunately for some components the predictions lead to overly conservative results which predict failures long before observations indicate.

The simplified assessment route is based on a shaken down, stabilised loop and does not consider evolution prior to or following this idealised cycle.

Creep FEA may also be used to determine elastic follow-up resulting from the interaction between the assessment location and the rest of the component / system (which consists of an extensive system of pipes). The elastic follow-up factor, Z, represents the increase in total strain compared to pure stress relaxation (Z=1). It is quantified by the ratio of creep strain to elastic strain during a dwell as follows:

$$Z = \frac{\Delta\bar{\varepsilon}_c}{\Delta\bar{\varepsilon}_{el}}$$

However, advancements in FEA mean that conservatism in the simplified assessment route can be reduced by calculating damage directly on a cycle by cycle basis. Therefore, three approaches can be defined for use of FEA:

1. FEA to provide stress input;
2. FEA to provide stress and elastic follow-up factor inputs;
3. FEA to calculate damage directly.

This paper compares the damage calculated directly from FEA (i.e. Approach 3) with that predicted by the traditional route (under Approach 1) for a case study.

COMPONENT AND LOADING

The component assessed in this case study is a ~2.5 inch diameter thin walled 316H austenitic stainless steel boiler tailpipe (within a system of tailpipes – see Figure 1) with a welded strap of cross-sectional dimensions ~1.5 inch x ~1 inch and length of 1.5 inch. The focus of this paper is the full penetration 316 weld at the strap to pipe connection, which is modelled with roughly a 45° capping profile. The location of the welded strap connection of most concern from creep-fatigue damage is shown in Figure 1.

The tailpipe is modelled using the following loads and boundary conditions:

- Negligible differential pressure (~1MPa);
- System moments due to deadweight;
- Long range displacements due to global thermal expansion of the system;
- Thermal expansion of the tailpipes.

The system is subjected to 30 load cycles whereby all thermal and pressure loads are cycled from a cold state (at 20°C).

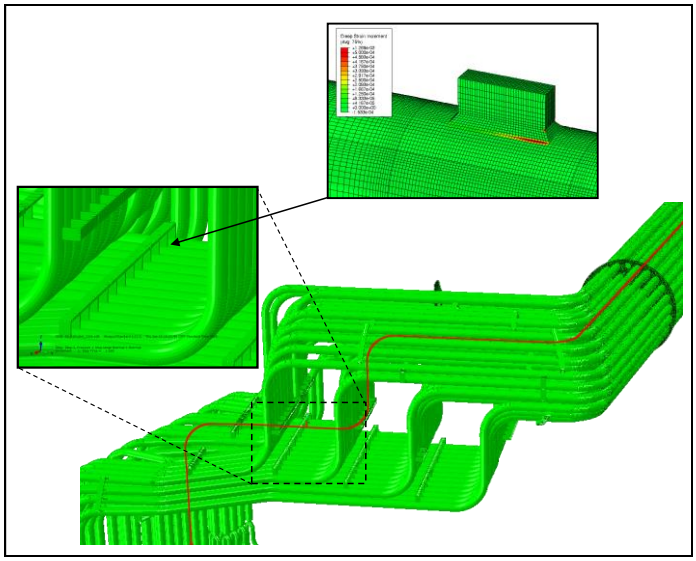

Figure 1: Boiler Tailpipe System with Assessed Connection Zoomed In

MATERIAL PROPERTIES

Homogenous (316H Parent) Material Properties

Physical material properties (thermal expansion and elastic properties) are extracted from R66 [2].

To model the elastic-plastic material response, a bi-linear kinematic hardening fit has been derived using the cyclic stress-strain properties (saturated) from R66 [2] as shown in Figure 2. The linear fit overestimates the stress range particularly at low plastic strain ranges and considering the majority of system loads are strain controlled this intentional conservatism leads to higher dwell stresses and consequently higher creep damage.

Creep deformation is based on the RCC-MR forward creep strain constitutive relation using a strain hardening formulation, that includes primary and secondary creep strain rates [2]. Re-priming of creep strain (i.e. re-setting creep strain to zero to allow the primary creep regime to be repeated) is assumed when reverse plasticity in a cycle exceeds 0.01% [2]. Uniaxial creep ductility values are extracted from R66 and are modified in the creep damage calculation to take account of multiaxial stress states via the Spindler fraction defined in R5 V2/3 [1]:

$$\frac{\bar{\varepsilon}_f}{\varepsilon_f} = \exp\left[p\left(1-\frac{\sigma_1}{\bar{\sigma}}\right)\right]\exp\left[q\left(\frac{1}{2}-\frac{3\sigma_H}{2\bar{\sigma}}\right)\right]$$

where $\bar{\varepsilon}_f$ and ε_f are the multiaxial and uniaxial creep ductilities respectively, σ_1, $\bar{\sigma}$ and σ_H are the maximum principal, equivalent and hydrostatic stresses respectively, and the constants p and q are derived from biaxial creep tests on the appropriate material.

The Spindler fraction input stresses can be obtained from the elastic FEA or more accurately from the same monotonic creep FEA as that used for determining the elastic follow-up factor. Alternatively, it may be possible to assume the stress state (e.g. biaxial at a free surface). The standard approach conservatively assumes that the most onerous stress state during the dwell period applies at all times.

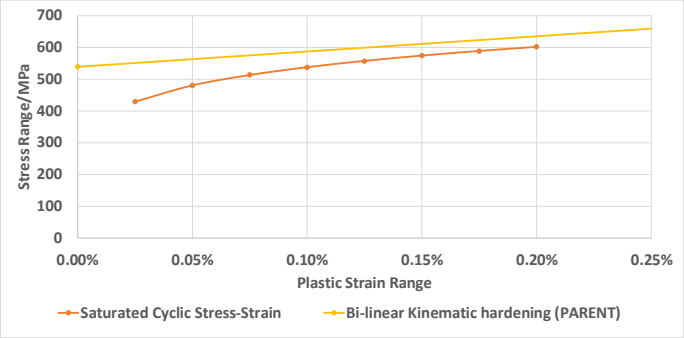

Figure 2: Bi-linear (Plastic) Fit to Saturated Cyclic Stress-Strain Data at 550°C

CREEP-FATIGUE DAMAGE CALCULATION

Defect initiation is assumed to occur only due to creep damage since fatigue is negligible in this example.

The creep damage per cycle, d_c, is calculated using ductility exhaustion as per R5 V2/3 [1]:

$$d_c = \int_0^{t_h} \frac{\dot{\bar{\varepsilon}}_c}{\varepsilon_f \times spindlerfraction} dt$$

where $\dot{\bar{\varepsilon}}_c$ is the instantaneous equivalent creep strain rate during the dwell period (which has total time, t_h). Once the damage value summed across each cycle reaches unity, then a failure event is conceded (e.g. defect / crack initiation).

Damage is not considered from residual weld stresses since in this case they are perturbed after the first load cycle and would not affect the comparison of subsequent cycles presented in this paper.

HOMOGENOUS MATERIAL FINITE ELEMENT ANALYSIS

Use in Traditional R5 V2/3 Assessments

The FEA results are used to output three values:

- Elastic stress range for the initial load cycle;
- Spindler fraction (equi-bi-axial in this case).

The R5 V2/3 procedure then conservatively calls for the following simplifications:

- Conversion of elastic stress range into elastic plastic stress range using Neuber estimation (this is based on a 'notch' like feature with a localised area of peak stress with an associated follow-up);
- The start of dwell stress for this representative cycle is based on cycle positioning relative to the shakedown yield limits (i.e. shakedown factor multiplied by yield strength) at each end of the cycle (cold and hot states);
- The same elastic stress range and thus start of dwell stress is used for all cycles (based on a stabilised shaken down loop);
- All load cycles are assumed to re-prime the creep strain if the cyclic reverse plasticity exceeds 0.01% (which is the case here);
- A constant elastic follow-up of 3 is used as per guidance in R5 V2/3 Appendix 8.

The elastic stress range from the FEA at the weld toe location is based on linearised values through the pipe wall. To account for the weld toe detail and material mismatch effects, the SCF and a WSEF are used to capture the local stress and strain ranges. The approach of using linearised stress ranges and SCF/WSEF factors are not used in this FEA based damage approach and instead stress ranges are used directly.

Modelling Approach for FEA Based Damage Prediction

The calculation of creep damage is undertaken every time increment for each element integration point within the FE model. The creep deformation is calculated via a FORTRAN user subroutine within the analysis whereby each load cycle is assumed to re-prime the creep strain rate. Spindler fraction and damage calculations are undertaken using a Python post-processing script. Figure 3 shows a contour of the predicted damage accumulated after 30 load cycles at the weld of interest.

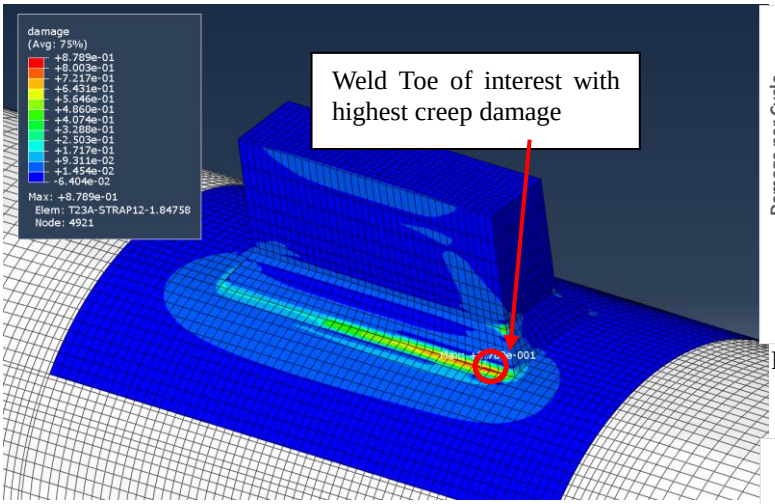

Figure 3: Creep Damage Contour at Assessed Connection

The FEA was run for 30 load cycles and the damage up to 100 cycles is extrapolated based on a power law trend of damage per cycle (see Figure 4). A comparison of the creep damage evolution, at the integration point predicted to have the highest creep damage after 30 load cycles, is compared to that from the traditional route and shown in Figure 4 and Figure 5. It is noted that the FEA model includes an inbuilt SCF due to the weld profile and the results from the traditional assessment presented here use the linearised stress range and an associated constant SCF for an undressed weldment based on R5 V2/3 Appendix 4.

It is observed that the creep damage calculated directly from the FEA is significantly higher during the initial cycles but the damage from each subsequent load cycle decreases leading to a significantly lower total damage after 100 cycles.

Figure 6 shows the evolution of the dominant stress component (hoop direction) demonstrating that it has shaken down. The Von Mises stress at the start of each load cycle is shown in Figure 7, reducing with each cycle compared to the fixed value used in the traditional route.

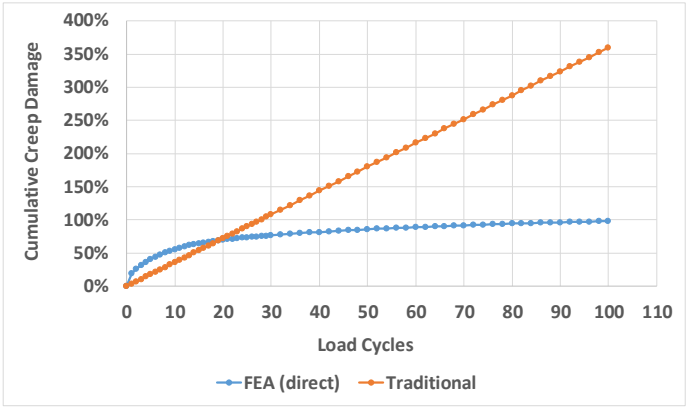

Figure 4: Evolution of Accumulated Creep Damage at Integration Point with Peak Total Creep Damage

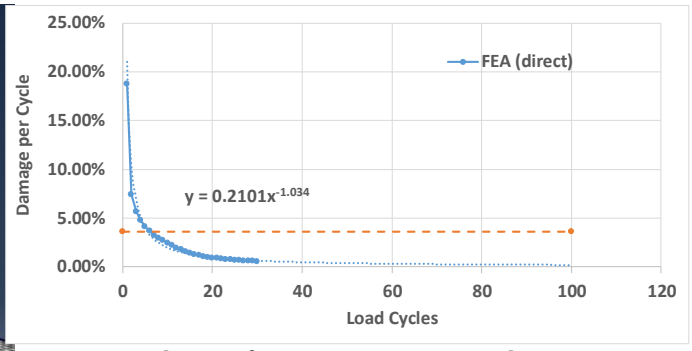

Figure 5: Evolution of Creep Damage per Cycle at Integration Point with Peak Total Creep Damage

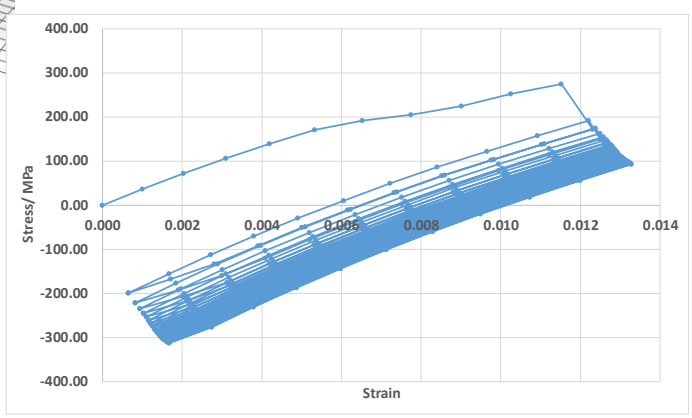

Figure 6: Evolution of Dominant Stress Component with each Cycle

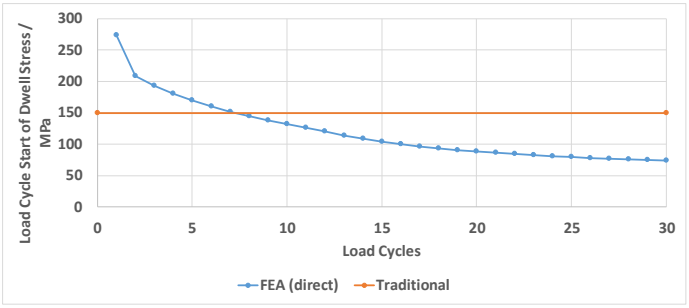

Figure 7: Evolution of Dominant Stress Component with each Cycle

Figure 8 shows the associated elastic follow-up (calculated using quantities accumulated in each dwell) indicating higher values from the FEA compared to the value of 3.0 used in the traditional route, prior to shakedown (roughly after eight cycles).

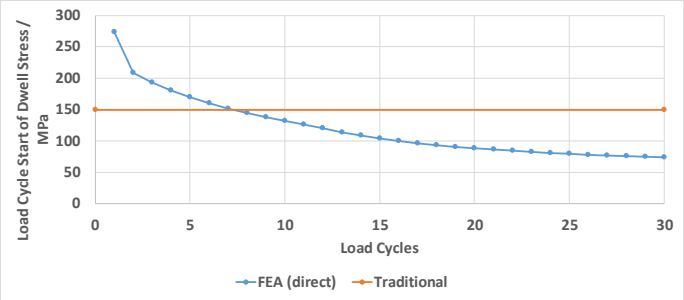

Figure 8: Evolution of Elastic Follow-Up with each Cycle (averaged per cycle)

Figure 9 shows the evolution of accumulated creep strain with creep re-priming assumed in all load cycles. Figure 10 demonstrates a significant effect on the overall damage from re-priming in the initial eight cycles.

Figure 9: Evolution of Accumulated Creep Strain

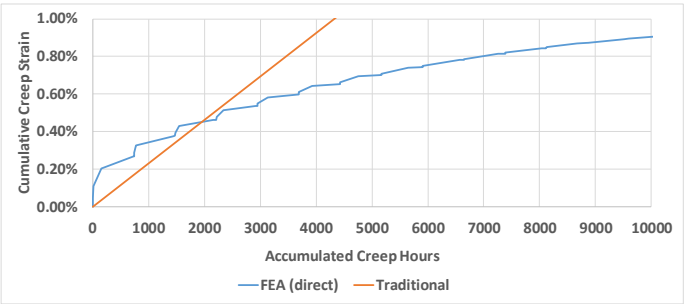

Figure 10: Evolution of Accumulated Creep Strain during the Initial Load Cycles

Figure 11 shows that the Spindler fraction reduces (i.e. the stress state tends to be hydrostatic) because of greater creep relaxation of the dominant stress component. The non-conservatism in the assumption used in the traditional assessment (a fixed fraction of ½) is small compared to the significant conservatisms in the traditional assessment shown by Figure 6 to Figure 10 for the start of dwell stress and assumption of creep re-priming in each load cycle.

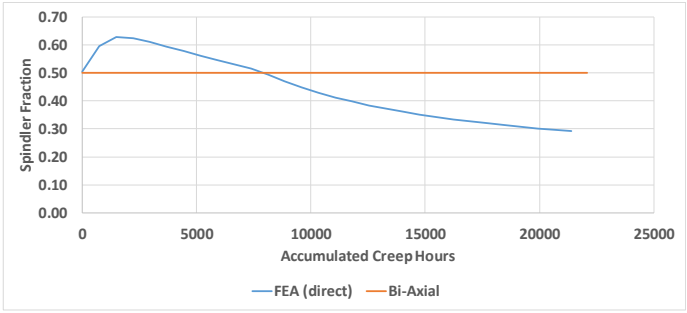

Figure 11: Evolution of Spindler Fraction

EFFECT OF MULTI-MATERIAL MODELLING ON DAMAGE

Homogenous Model Limitation

A homogenous material FE model does not account for the material mismatch between the weld, heat affected zone (HAZ) and parent materials. This mismatch could potentially induce higher stresses and follow-up at the interface and subsequently higher creep damage. This effect will be assessed in the following section.

Weld Material Modelling

The material properties considered to investigate the effect of weldment property mismatch are:

- Elastic properties;
- Cyclic stress-strain properties (saturated cycle);
- Creep deformation properties.

The thermal expansion and creep ductility properties are unchanged.

Mismatch for each material property is initially assessed separately to determine significance on the predicted creep damage. Six analyses are undertaken where the weld material is the same as the parent material model except for:

- Higher yield limit but unchanged plastic curve slope (Case a);
- Lower yield limit but unchanged plastic curve slope (Case b);
- Higher (ten times parent) creep deformation rate (Case c);
- Lower (tenth of parent) creep deformation rate (Case d);
- Lower elastic modulus from R66 [2] for 316 weld (Case e);
- Conservative combination of case a + case d + case e (Case f).

Figure 12 shows the stress-strain curves used to represent the weld material in cases a, b, e and f.

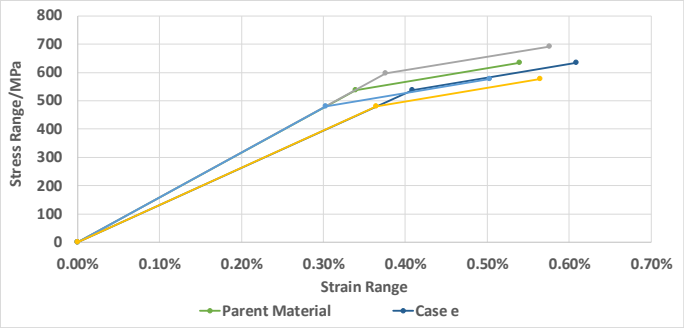

Figure 12: Stress-Strain Curves used for the Modelled Weld Material for all Cases at 550°C

Figure 13 shows a comparison of the best estimate stress-strain behaviour for the parent and weld materials at 550°C assuming saturated cyclic behaviour. Considering they are broadly similar and for simplicity, use of the same slope from the bi-linear kinematic hardening fit from the parent material is judged to be representative for the weld material.

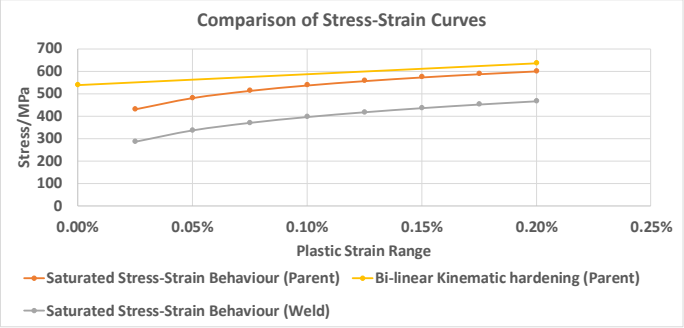

Figure 13: Comparison of Saturated Stress-Strain Behaviour for Parent and Weld Materials at 550°C

Predicted Creep Damages

Figure 14 shows the predicted evolution of creep damage at the integration point with the highest total creep damage (after 30 load cycles). The peak damage occurs in the parent material in all cases. The highest damage occurs in the same element except for cases e and f which occur a few elements away.

The following observations are made:

- Insignificant effect on damage from changing the weld material yield limit (cases a and b);
- Insignificant increase in damage from lower creep rate in the weld (case d);
- Reduction in damage from higher creep rate in the weld (case c)
- Significant increase in damage due to the weld material elastic modulus (case e);
- Consideration of creep, elastic and plastic mismatch (case f) is dominated by the elastic behaviour mismatch.

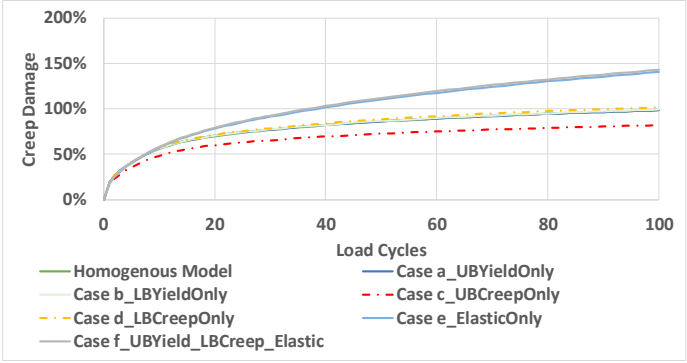

Figure 14: Predicted Creep Damage in the Parent Material for different Modelled Weld Cases

Figure 15 shows the equivalent cumulative creep strain over the initial load cycles indicating that cases a, b and d have similar values to that of the homogenous model. Assuming a higher creep rate in the weld (case c) leads to lower elastic follow-up in the parent material thus reduced creep strains. When considering the (lower) elastic modulus of the weld material (i.e. cases e and f), stresses are reduced (given that the thermal loads are strain controlled) and although elastic follow-up increases, overall there is a reduction in creep strain.

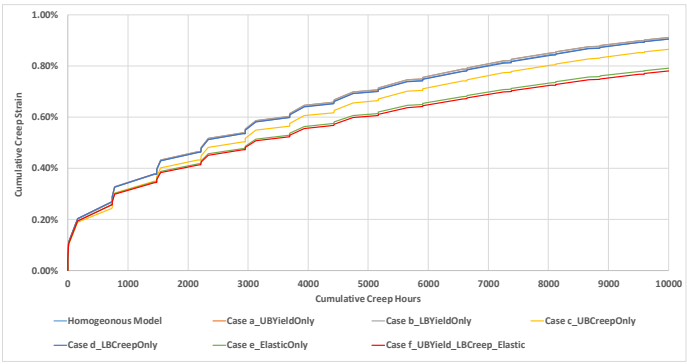

Figure 15: Predicted Cumulative Creep Strain in the Parent Material for different Modelled Weld Cases

Figure 16 shows the variation in Spindler fraction at the end of each load cycle indicating a similar curve for cases a, b and d to that of the homogenous model. Using a higher creep rate in the weld (case c) leads to reduced follow up in the parent and higher increase in Spindler fraction in the first few cycles but a similar rate of reduction compared to the homogenous model. For cases e and f, the Spindler fraction does not increase in the initial cycles but instead only reduces at a rate similar to the homogenous model.

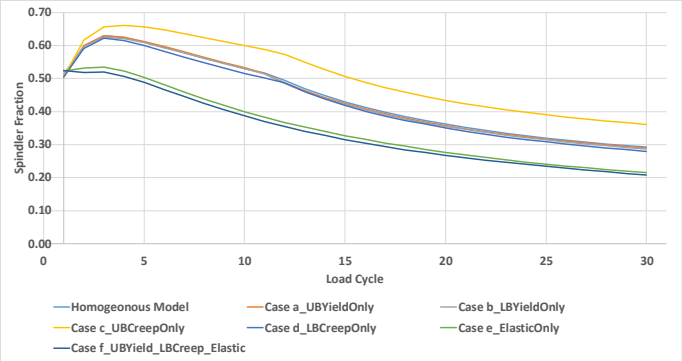

Figure 16: Predicted Spindler Fractions for different Modelled Weld Cases

Comparison to Traditional Route

In line with the traditional route in R5 V2/3 for weldments, the load cycle strain range is factored by a WSEF to account for material mismatch effects and geometric stress concentration. Figure 17 compares the predicted creep damage using the WSEF for full penetration T-joint welds, compared to the results from the multi-material FEA for case f.

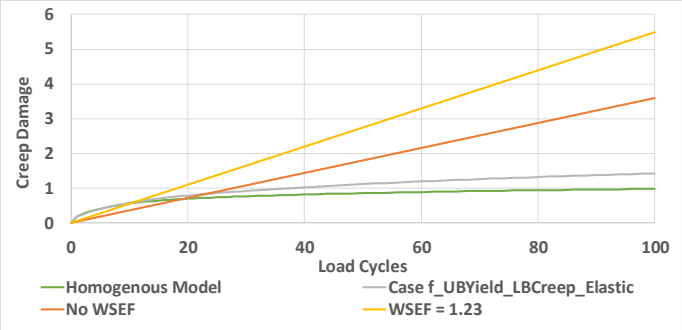

Figure 17: Evolution of Creep Damage at Peak Location considering Material Mismatch Effects in FEA compared to the WSEF Approach

It is observed in Figure 17 that the relative increase in damage after 100 cycles is similar between the traditional route with and without the WSEF, and that obtained directly from the homogenous and multi-material FEA. Unlike the traditional route, whereby the relative increase is constant (due to a constant WSEF), the multi-material FEA results in an increasing effect with increasing number of load cycles as shown in Figure 18.

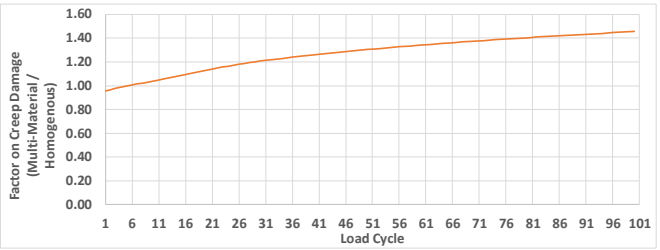

Figure 18: Factor on Creep Damage between the Multi-Material and Homogenous FEA

LIMITATIONS AND UNCERTAINTIES

Weld Profile Uncertainty

There is often uncertainty in the exact weld profile, which influences the SCF at the toe and whether failure occurs through the weld throat or from the toe. Considering that high localised stresses at the weld toe may lead to plasticity, this inhibits the effect of the SCF and thus uncertainty in this regard is minimal. It is unlikely that a well manufactured weld would have a concave shape, and as such a 45° profile is judged to be representative, and therefore defect initiation is most likely to originate at the weld toe.

Evolution of Stress-Strain Behaviour

The stress-strain curves used are based on saturated cyclic behaviour which is conservative for determining start of dwell stresses and consequently creep damage. No consideration has been taken for the following effects:

- Evolutionary hardening (e.g. from initial (monotonic) state to saturated);
- Thermal recovery of hardening during dwells (which restricts the amount of hardening per cycle);

Figure 19 shows stress-strain curves assuming monotonic or saturated behaviour marking a significant difference in the stress ranges (roughly double) for a given strain range. For the initial load cycles, the stress-strain behaviour would actually be more similar to the monotonic behaviour, which would result in a lower start of dwell stress and significantly reduce the initial damage rate.

It is a simplification to treat creep and plastic behaviour separately and this can result in convergence problems in the FEA when the plastic strains are high. To avoid this issue, a unified creep-plasticity model is recommended.

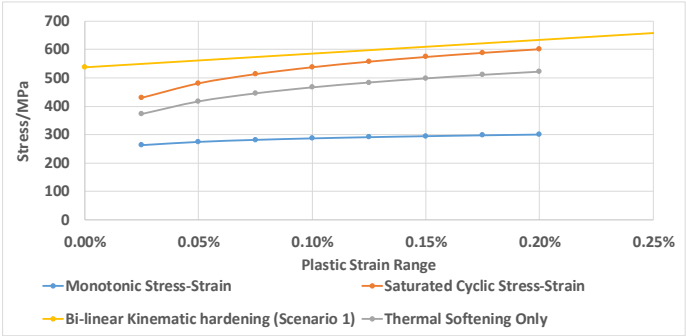

Figure 19: Effect of Thermal Recovery on Hardening

Material Boundaries

A simplification is undertaken whereby the parent and weld material are modelled with a distinct boundary (i.e. there is no graduation). The HAZ is judged to behave similarly to the parent material and is not represented separately. Since the model-fitted cyclic stress-strain curves (at saturation) for both

the weld and parent materials are broadly similar (see Figure 13) not modelling their interface is not judged to be a limitation considering the level of plasticity exhibited. Although when considering the evolution of stress-strain data, this limitation becomes more critical as initially the weld material is relatively harder but softens and vice versa for the parent material.

It is noted that the creep deformation rate of the weld material can be orders of magnitude less than the parent material and as such it is expected that significantly higher elastic follow-up would be observed in the parent material and subsequently higher creep damage. Since the WSEFs in R5 V2/3 were derived from fatigue tests only and therefore do not account for creep behaviour mismatch, the comparison between the traditional route (using WSEFs) and the multi-material FEA for cases a, b and e is like for like.

Creep Ductility

The creep damage is calculated based on a creep ductility which does not account for strain rate effects whereby higher rates is associated with higher ductility allowables. Use of strain rate effects could potentially reduce the creep damage from the initial cycles, where creep strain rates are highest.

CONCLUSION

The creep damage predicted directly from FEA is shown to be significantly lower than that predicted by the traditional R5 V2/3 route. This is due to the reduction in start of dwell stress and hence creep damage in each subsequent load cycle as opposed to a single representative cycle. It is noted that the R5 V2/3 procedure is intended to be conservative and this paper highlights the areas in which conservatisms may be relieved.

The parent-weld interaction is observed to be dominated by the mismatch in elastic modulus. Despite predicting lower creep strains (due to reduced stresses) and higher elastic follow-up compared to the homogenous model, the lower Spindler fraction is such that the creep damage increases.

ACKNOWLEDGMENTS

Acknowledgement for the cooperation from EDF Energy.

REFERENCES

[1] ‘Creep-Fatigue Crack Initiation Procedure for Defect-Free Structures’, *Assessment Procedure for the High Temperature Response of Structures*, R5 Volume 2/3, Issue 3 Revision 002 (2014). EDF Energy Nuclear Generation Ltd, UK.

[2] AGR Materials Data Handbook R66, Revision 010 (2016), EDF Energy Nuclear Generation Ltd., UK.

[3] ‘R5 High Temperature Creep-Fatigue Life Assessment for Austenitic Weldments’, D M Knowles, *Procedia Engineering*, Volume 86, Pages 315-326, 2014.